Applied Clay Science 132–133 (2016) 261–266

Contents lists available at ScienceDirect

Applied Clay Science

journal homepage: www.elsevier.com/locate/clay

Research paper

Structure and thermal stability of organo-vermiculite

Xiaoli Su [a,b,c], Lingya Ma [a,c], Jingming Wei [a], Runliang Zhu [a,*]

[a] Guangdong Provincial Key Laboratory of Mineral Physics and Material/CAS Key Laboratory of Mineralogy and Metallogeny, Guangzhou Institute of Geochemistry, Chinese Academy of Sciences, Guangzhou 510640, China
[b] School of Material Science and Engineering, Jingdezhen Ceramic Institute, Jingdezhen 333001, China
[c] University of Chinese Academy of Sciences, Beijing 100049, China

ARTICLE INFO

Article history:
Received 23 March 2016
Received in revised form 8 June 2016
Accepted 17 June 2016
Available online 22 June 2016

Keywords:
Organo-vermiculite
Surfactant modification
Interlayer structure
Thermal stability

ABSTRACT

In this study, organo-vermiculites (HEVrm) were prepared by modifying expanded vermiculite (EVrm) with different amounts of surfactant (hexadecyltrimethyl ammonium bromide, HDTMAB). The obtained HEVrm were characterized by using X-ray diffraction (XRD), Fourier transform infrared spectroscopy (FTIR), and thermogravimetric analysis (TG). Instead of a gradual increase of the basal spacing for organo-montmorillonite (OMt) as reported in literatures, a one-stepped increase of the basal spacing was observed for HEVrm. As such, the intercalation of surfactant into the interlayer space of EVrm is not homogeneous. In particular, only part of the interlayer spaces of EVrm were intercalated by surfactants at low HDTMAB concentration; with the increase of surfactant concentration, more and more interlayer spaces were intercalated, reaching a "saturation" state at last. The intercalated surfactant adopted a paraffin-monolayer arrangement with *all-trans* conformation within the interlayer space. The decomposition temperature of the intercalated surfactant in HEVrm is very similar to that of neat surfactant. The protection of the clay mineral layers for the thermal stability of the intercalated surfactant is not obvious, which is very different from that for OMt. This may be due to the one-stepped increase of the basal spacing in HEVrm with relatively large interlayer height. These findings are of high importance for preparation and application of HEVrm.

1. Introduction

During the recent decades, organoclays (OC) have attracted great attentions due to their extensive application in various fields such as adsorbents for organic contaminants and as fillers of clay-based polymer nanocomposites (He et al., 2005a; Liu et al., 2011; Zhu et al., 2011; Cai, 2012; Zhu et al., 2012b; Bergaya and Lagaly, 2013; Wang et al., 2013). OC showed significantly improved adsorption capacity towards organic contaminants in comparison with that of the original clay minerals (He et al., 2006); while clay-polymer complexes displayed increased strength and heat resistance, decreased gas permeability and flammability (Tjong and Meng, 2003). These improvements are highly dependent on the structure and property of OC (He et al., 2014), including basal spacing, loaded surfactant quantity, and existing styles of surfactant (i.e., cation or molecule). OC are usually obtained by introducing cationic surfactants into the interlayer space of clay minerals via cation exchange with previously existing interlayer cations (Bergaya and Lagaly, 2011). Up to now, the most widely used clay mineral is montmorillonite (Mt), which has a relatively low charge density (0.2–0.6 eq./formula unit) (Zhu et al., 2003; He et al., 2010).

A number of studies have demonstrated that the basal spacing of organo-montmorillonites (OMt) increased with the increase of loaded surfactant quantity. A maximum basal spacing could reach when the amount of the loaded surfactant is >1 times of the clay mineral's cation exchange capacity (CEC) (Zhu et al., 2012a). In this case, both surfactant cation and molecule (ion-pair) can be intercalated into the interlayer space, resulting in significant effects on the structure and property of the resultant OMt (Xi et al., 2007a). For instance, the intercalation of surfactant molecule could dramatically decrease the thermal stability of OMt (He et al., 2005c).

Basal spacing and organic carbon content are of high importance in the application of OC, which strongly depend on the layer charge density of clay minerals (He et al., 2010). Vermiculite (Vrm) is a 2:1 type phyllosilicate with higher layer charge density (0.6–0.9 eq./formula unit) than Mt (0.2–0.6 eq./formula unit) (He et al., 2005c). The Vrm layer is composed of one Mg-$O_4(OH)_2$ octahedral sheet sandwiched between two opposing Si-O tetrahedral sheets. The layer charge mainly arises from the substitution of Al^{3+} for Si^{4+} in tetrahedral sheet (Brigatti and Theng, 2013), which is balanced by interlayer exchangeable cations (e.g., Mg^{2+}, Na^{+}, Ca^{2+}, and K^{+}). Due to high charge density, Vrm may adopt more cationic surfactant than Mt within its interlayer space (Mittal, 2012b). Thus, organo-vermiculite (HEVrm) with high organic carbon content and large basal spacing can be obtained via

* Corresponding author.
E-mail address: zhurl@gig.ac.cn (R. Zhu).

http://dx.doi.org/10.1016/j.clay.2016.06.011
0169-1317/

Table 1
The amounts of the added surfactant in preparation solution and the loaded surfactant in HEVrm, and basal spacing of the resultant HEVrm.

Samples	Amount of added surfactant (CEC)	Amount of loaded surfactant (CEC)	d (nm)
EVrm	0	0	1.48
$HEVrm_{0.2}$	0.2	0.18	2.71
$HEVrm_{0.4}$	0.4	0.38	2.76
$HEVrm_{0.6}$	0.6	0.57	2.77
$HEVrm_{0.8}$	0.8	0.82	2.80
$HEVrm_{1.0}$	1.0	1.13	2.82
$HEVrm_{1.5}$	1.5	1.43	2.88
$HEVrm_{2.0}$	2.0	1.62	2.94
$HEVrm_{3.0}$	3.0	1.37	2.88

exchange between the interlayer cations and cationic surfactants (e.g., quaternary ammonium), which has potential application as effective adsorbent towards organic contaminants, and as filler for polymer-clay nanocomposites (Valaskova et al., 2009; Dultz et al., 2012; Placha et al., 2014). Thermal stability of OC is a critical factor for preparation and application of clay-based polymer nanocomposites, as they are prepared by mixing polymers and OC at high temperature and sheared in a compounder (Mittal, 2012a). A considerable body of literature has reported the investigations of the thermal stability of OC under different conditions on OMt (Hedley et al., 2007), much less on HEVrm.

In this study, HEVrm were prepared with expanded vermiculite (EVrm) under different concentrations of hexadecyltrimethyl ammonium bromide (HDTMAB). A combination of characterization techniques, including thermogravimetric analysis (TG), X-ray diffraction (XRD), and Fourier transform infrared spectroscopy (FTIR), was applied to investigate the structure and thermal stability of the resulting HEVrm. The obtained insights are of high importance for preparation and application of OC.

2. Experimental

2.1. Materials

EVrm was obtained from Shijiazhuang, Hebei Province, China. The chemical composition (wt%) of EVrm is as follows: SiO_2 28.37%, Al_2O_3 19.6%, Fe_2O_3 5.85%, CaO 7.21%, MgO 27.05%, Na_2O 0.21%, K_2O 1.44%, TiO_2 0.85%, L.O.I. 11.96%. The sample was dried at 80 °C and ground through a 100 mesh sieve. The cation exchange capacity (CEC) of EVrm is 122.4 mmol/100 g, determined by the adsorption of $[Co(NH_3)_6]^{3+}$ (Wang et al., 2015). HDTMAB ($C_{19}H_{42}NBr$, FW: 364.446) with a purity of 99% was provided by Nanjing Robiot Co., Ltd., China. All these materials were used as received without any further treatment.

2.2. Synthesis of organo-vermiculite

HEVrm were prepared according to the following procedure. 5.0 g of EVrm was dispersed in 200 mL of distilled water under stirring for 10 min. A pre-dissolved stoichiometric amount of HDTMAB solution was slowly added into the EVrm dispersion. The dispersion was stirred at 80 °C and 800 rpm for 4 h, and aged at 80 °C for 48 h. The amounts of HDTMAB added were 0.2, 0.4, 0.6, 0.8, 1.0, 1.5, 2.0, and 3.0 CEC of EVrm, respectively. The obtained products were washed with distilled water until bromide anion free, which were determined by $AgNO_3$ solution, and then dried at 80 °C for about 12 h. The obtained samples were ground in an agate mortar for further investigation. The HDTMAB modified EVrm are denoted as $HEVrm_x$, where *x* stands for the HDTMAB concentration under which HEVrm was prepared.

2.3. Characterization methods

Elemental analysis of carbon was conducted on an Elementar Vario EL III Universal CHNOS Elemental Analyzer. About 5 mg of sample was placed in a tin boat and burnt under pure O_2 environment. Concentrations of the resulting CO_2 and N_2 were analyzed as a function of the thermal conductivities of the produced CO_2 and NO_x gases. The original EVrm has an organic-carbon content of 0.28%, and the loaded surfactant amount in HEVrm was calculated by subtracting the organic-carbon content (0.28 wt%) in the original EVrm from the measured organic-carbon contents value (f_{oc}) in HEVrm.

The X-ray diffraction (XRD) patterns of the samples were recorded on a Bruker D8 Advance diffractometer with Ni-filtered Cu Kα radiation at 40 kV and 40 mA between 3° and 12° at a scan rate of 1° (2θ) min^{-1}. In order to investigate the intercalation processes, the XRD patterns ($2\theta = 5–7°$) of the HEVrm prepared at 0.2, 0.4, 0.6, and 0.8 CEC were fitted by the PEAKFIT using a Gauss-Lorentz function, and the position and area of reflections were obtained. The goodness-of-fit (R^2) values for all reflections are ≥0.99.

Fourier-transform infrared (FTIR) spectra of the samples were obtained on a Bruker vertex-70 spectrometer. The specimens were prepared for measurements by mixing 0.9 mg of sample powder with 80 mg of KBr and pressing the mixture into a pellet. The spectra were recorded at 25 °C over the range of 4000–600 cm^{-1} with 64 scans and a resolution of 4 cm^{-1}.

Thermogravimetric (TG) analysis was performed on a Netzsch STA409PC instrument operating from 30 °C to 1000 °C under a high

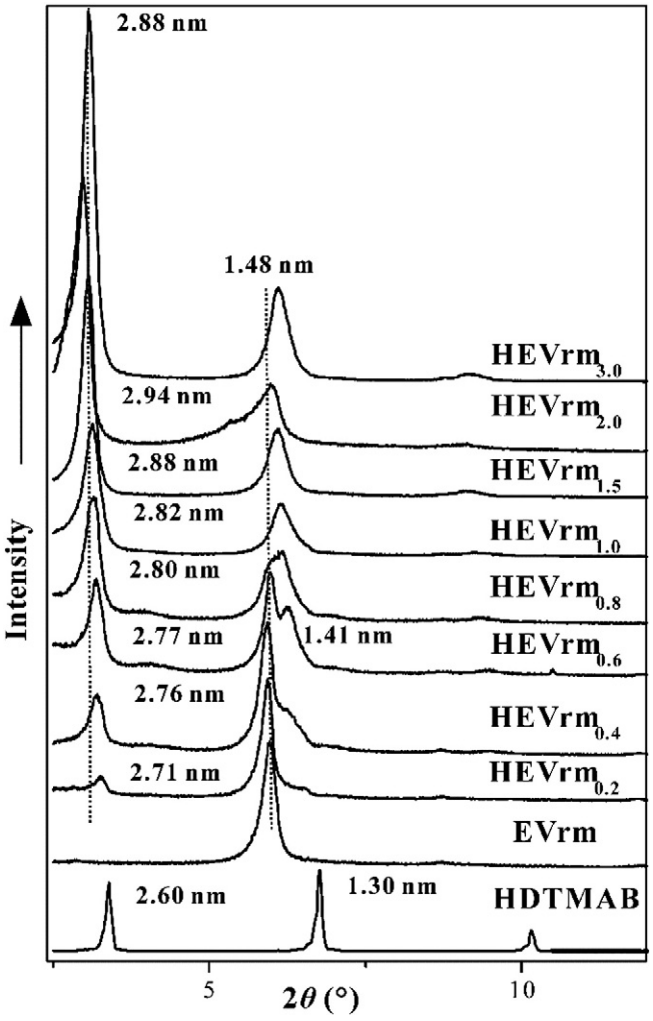

Fig. 1. XRD patterns of EVrm, HDTMAB and HEVrm samples.

purity flowing nitrogen atmosphere (60 cm^3/min). About 10 mg of finely ground sample was heated in a corundum crucible. The differential thermogravimetric (DTG) curve was derived from the TG curve.

3. Results and discussion

3.1. Interlayer structure of HEVrm

The amounts of the added surfactant in preparation solution and the loaded surfactant in the resultant HEVrm are tabulated (Table 1). The amounts of loaded surfactant are close to that of the added surfactant in preparation solution below 1.0 CEC, while the loaded amounts are less than that of the added above 1.0 CEC. The quantity of the loaded surfactant reached a maximum when the added surfactant concentration is above 1.5 CEC, which is similar to OMt (He et al., 2005b; Zhu et al., 2012a). Generally, when the added surfactant concentration is lower than 1.0 CEC, the cationic surfactants enter the interlayer space of clay minerals via cation exchange whereas both surfactant cations and molecules can be intercalated into the interlayer spaces when the added surfactant concentration is above 1.0 CEC (He et al., 2005a).

In the case of OMt, with the increase of the loaded surfactant quantity, a gradual increase of the basal spacing of the resultant OMt could be observed, and the maximum can be reached when the clay minerals are "saturated" with surfactants (He et al., 2010). Interestingly, a one-stepped increase of the basal spacing in HEVrm was observed in this study, instead of a gradual increase for OMt reported in literature (He et al., 2005a, 2010). The XRD pattern of EVrm displays a characteristic (002) reflection at 5.9° 2θ (d_{002} = 1.48 nm) (Fig. 1). After modifying EVrm with HDTMAB at 0.2 CEC, the obtained $HEVrm_{0.2}$ exhibits a strong reflection at 1.48 nm with a weak one at 2.71 nm (Fig. 1). With the increase of the added surfactant concentrations, the intensity of the reflection at 2.7–2.9 nm, the maximum basal spacing, significantly increased. Meanwhile, the intensity of the reflection at ~1.48 nm increased with the increase of the added surfactant concentration at 0.2–0.8 CEC. Interestingly, this reflection (2θ = 5–7°) is obviously asymmetric for HEVrm prepared at 0.2–0.8 CEC and two well resolved reflections at 1.48 and 1.41 nm, respectively, were recorded in XRD pattern of $HEVrm_{0.6}$. The deconvolutions of the reflections at the 2θ range of 5–7° for $HEVrm_{0.2}$, $HEVrm_{0.4}$, $HEVrm_{0.6}$, and $HEVrm_{0.8}$ show two reflections at 1.36–1.42 and 1.48–1.49 nm (Fig. 2 and Table 2), respectively. With the increase of surfactant concentration, the intensity of the reflection at 1.36–1.42 nm increased whereas that at 1.48–1.49 nm decreased. The former might be ascribed to the second-order reflection, corresponding to the first-order reflection of HEVrm at ~2.80 nm, while the latter is due to the basal reflection of Vrm. This suggests that the intercalation of surfactant in Vrm interlayer space is not homogeneous, i.e., only part of the interlayer spaces were intercalated by surfactants at low HDTMAB concentration. With the increase of surfactant concentration, more and more interlayer spaces were occupied by surfactant and reached a "saturation" state at last. According to the basal spacing of HEVrm (2.7–2.9 nm) and the layer thickness of Vrm (0.92 nm) (Walker, 1949), the interlayer height of the resultant HEVrm is about 1.8–1.9 nm. This implies that a paraffin-monolayer arrangement was adopted for the intercalated surfactant within the interlayer space of Vrm (Zhu et al., 2003).

As reported in previous studies, a gradual increase of the basal spacing in HDTMAB modified smectite group minerals was observed and a series of arrangement models have been proposed with the increase of surfactant loading, such as lateral-monolayer, lateral bi-layer, paraffin-monolayer, and paraffin-bilayer (Zhu et al., 2008, He et al., 2014). Different from smectite group minerals, however, only one kind of arrangement model (i.e., paraffin-monolayer) exists in HDTMAB modified Vrm, as was suggested by the abrupt increase of the basal spacing of those expanded interlayers, i.e., from 1.48 nm for Vrm to 2.7–2.9 nm for HEVrm. This may be due to the high layer charge density and the charge distribution on Si-O tetrahedral sheet in Vrm, which is resulted from the substitution of Al^{3+} for Si^{4+}. During the exchange of interlayer cations by cationic surfactants, the repulsive forces (between the two neighboring Vrm layers with high negative charge density) may drive the Vrm layers apart, resulting in a prominent increase of the interlayer

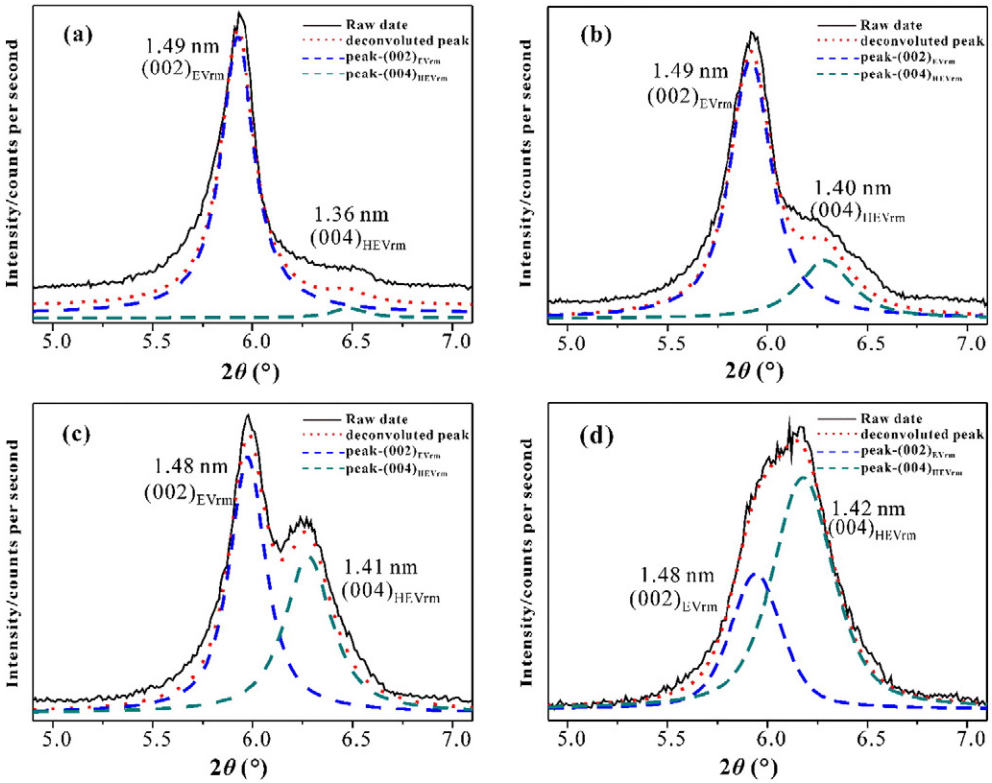

Fig. 2. XRD patterns of HEVrm and their deconvolutions in the 2θ ranges of 5–7°: (a) $HEVrm_{0.2}$, (b) $HEVrm_{0.4}$, (c) $HEVrm_{0.6}$, and (d) $HEVrm_{0.8}$.

height. Meanwhile, the positively charged amine group (i.e., the "head" of surfactant) was fixed on the Vrm layer surface through the strong electronic interaction between the positively charged "head" and negatively charged layer, and the hydrophobic alkyl chain orientation radiated away (He et al., 2004a), resulting in the paraffin-monolayer arrangement. On the other hand, the van der Waals forces among alkyl chains maintain the ordered *all-trans* conformation for the intercalated surfactant (He et al., 2004b), which is well evidenced by the FTIR spectra of HEVrm (Fig. 3).

The antisymmetric (ν_{as}) and symmetric stretching (ν_s) modes of CH_2 in alkyl chain of surfactant are sensitive to the conformation of the intercalated surfactant in OC Vaia et al., 1994; He et al., 2004b). Previous FTIR studies of OMt demonstrated that the frequency of both antisymmetric and symmetric CH_2 stretching modes for the intercalated surfactants strongly depended on its packing density in the interlayer space (He et al., 2004b). In the case of high surfactant loading, the frequencies of the CH_2 stretching vibrations are close to those of the pure surfactant, corresponding to an essentially *all-trans* conformation; whereas the frequency significantly shifts to high wavenumber for the samples with low surfactant loading, which could be attributed to *gauche* conformers in the alkyl chain (Zhu et al., 2005). As shown by the FTIR spectra of HDTMAB and the resultant HEVrm, the pure HDTMAB displays two intense vibrations at about 2918 and 2850 cm^{-1} (Fig. 3), corresponding to antisymmetric and symmetric stretching modes of CH_2 in alkyl chain, respectively. All the HEVrm samples also display two similar prominent vibrations at approximately 2918 and 2850 cm^{-1}, which is completely different from those of HDTMAB modified Mt, implying that the intercalation process of surfactant for Vrm is different from that for Mt. An integration of XRD and FTIR results suggests that the intercalation of HDTMAB for Vrm is one-stepped rather than stepwise. In other words, part of the interlayer spaces were intercalated at low surfactant concentration, reaching a maximum basal spacing with a paraffin-monolayer arrangement; and with the increase of surfactant loading, more and more interlayer spaces were occupied by surfactant, reaching a "saturation" at above 1.5 CEC.

3.2. Thermal stability of HEVrm

The TG and DTG curves of EVrm, HDTMAB, and HEVrm are recorded (Fig. 4), and the mass losses of these samples at different stages during heating treatment are summarized (Table 3). The mass losses of EVrm occurred at 30–210 °C are attributed to the removal of surface-adsorbed water and interlayer water associated with interlayer cations, respectively. The mass loss of dehydroxylation occurred at 600–810 °C, and the mass losses at 810–920 °C correspond to phase transformation (He et al., 2003; Perez-Maqueda et al., 2003; Huo et al., 2012). For neat HDTMAB, the mass loss at about 266 °C, corresponds to its decomposition (Fig. 4b).

After modifying EVrm with surfactant, prominent changes can be observed in the TG and DTG curves of HEVrm (Fig. 4). The mass loss at 30–150 °C, corresponding to the removal of surface adsorbed water, dramatically decreases with the increase of surfactant loading, which suggests an increase of hydrophobicity of EVrm surface after surfactant modification (Holesova et al., 2014). The mass loss at 150–210 °C, corresponding to the removal of the interlayer water associated with the interlayer cations (e.g., Mg^{2+} and Ca^{2+}), also decreases with increasing surfactant loading, which was resulted from the replacement of interlayer cation by surfactant cation. This mass loss disappeared when the surfactant concentration is above 1.0 CEC, implying an almost complete replacement of interlayer cation by surfactant.

The mass losses of HEVrm corresponding to the decomposition of the loaded surfactant occur at 210–500 °C (Xie et al., 2001, 2002). The prominent mass loss at ca. 266 °C should be attributed to the decomposition of intercalated surfactant cations, which is similar to the decomposition temperature of neat surfactant. This is very different from the case of surfactant modified Mt (Ma et al., 2014), where the decomposition temperature of the intercalated surfactant cation is significantly higher than that of neat surfactant (Zhu et al., 2011; Ma et al., 2015). It is noteworthy that, for OMt prepared at low surfactant concentration (e.g., 0.2 CEC), the interlayer height of the resultant OMt (approximately 0.4 nm) (Zhu et al., 2003; He et al., 2010) is much smaller than that of the corresponding $HEVrm_{0.2}$ in the present study (approximately 1.79 nm). In this case, the cationic surfactants in the interlayer space of OMt are lying flat, making maximum contact with the siloxane surface, and thus stabilize the intercalated surfactant. However, in the case of HEVrm at low HDTMAB concentration, the intercalated surfactant cations adopt a paraffin-monolayer arrangement within the interlayer space. The alkyl chain orientation radiating away from the Vrm surface results in weak interaction between surfactant and Vrm surface, and a relatively strong interaction among the alkyl chains of surfactant. Accordingly, the thermal stability of the intercalated surfactant in HEVrm is similar to that of the pure solid compound. This suggests

Table 2
The relative area of (002) reflection for vermiculite ($(002)_{EVrm}$) and (004) reflection of HEVrm ($(004)_{HEVrm}$) deduced from the deconvolution of the reflection at 5–7° (2θ).

Samples	Peak	Area percentage (%)	d(nm)
$HEVrm_{0.2}$	$(002)_{EVrm}$	97.07	1.49
	$(004)_{HEVrm}$	2.92	1.36
$HEVrm_{0.4}$	$(002)_{EVrm}$	77.89	1.49
	$(004)_{HEVrm}$	22.11	1.40
$HEVrm_{0.6}$	$(002)_{EVrm}$	56.10	1.48
	$(004)_{HEVrm}$	43.90	1.41
$HEVrm_{0.8}$	$(002)_{EVrm}$	68.07	1.48
	$(004)_{HEVrm}$	31.92	1.42

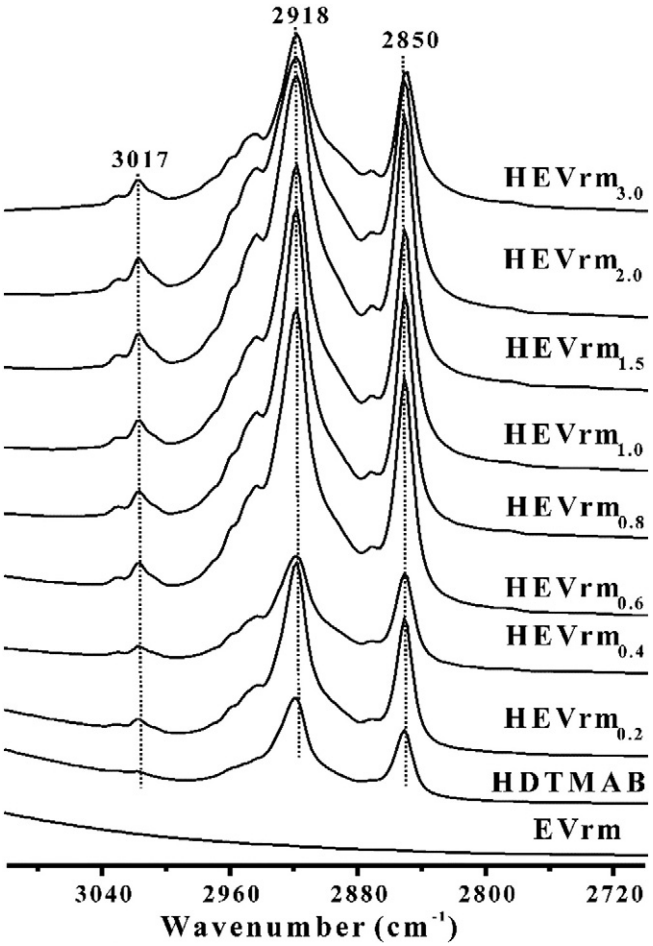

Fig. 3. Infrared spectra of EVrm, HDTMAB and HEVrm samples.

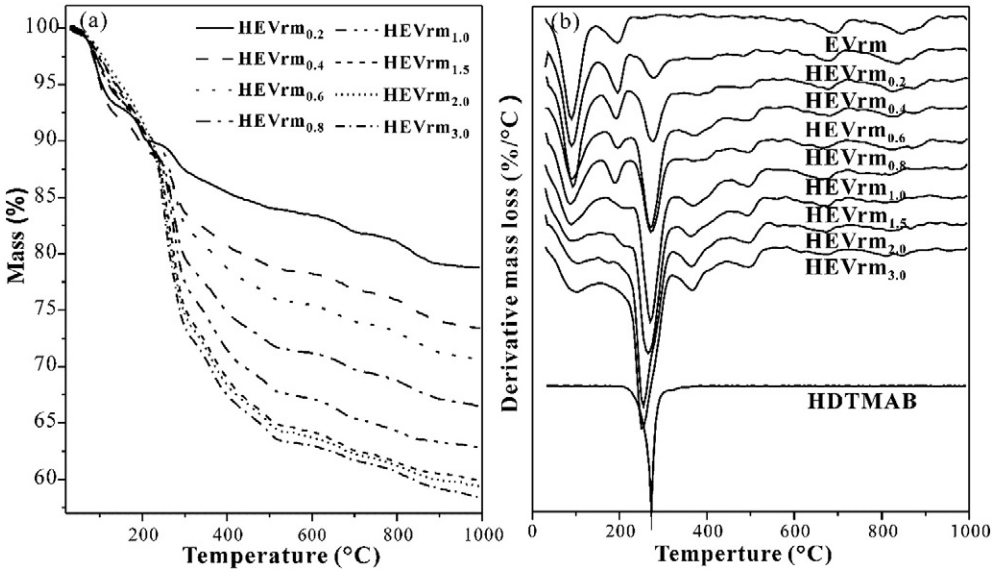

Fig. 4. (a) TG and (b) DTG curves of EVrm, HDTMAB and HEVrm samples.

that the protection of the intercalated surfactants by clay mineral layer only happens in the OC with relatively small interlayer height, and this phenomenon also can be found in literature, despite that it was not pointed out (He et al., 2005a; Park et al., 2012). With the increase of surfactant loading, the total mass loss corresponding to the loaded surfactant increased from 6.1% for $HEVrm_{0.2}$ to 26.2% for $HEVrm_{3.0}$, and finally reached a maximum in $HEVrm_{2.0}$ and $HEVrm_{3.0}$, consistent with the results of XRD analysis. Note that the DTG peaks at ~260 °C for $HEVrm_{2.0}$ and $HEVrm_{3.0}$ are obviously asymmetric, resulting from the decomposition of the intercalated surfactant molecules (i.e., ionic pairs) loaded via van der Waals force (Xi et al., 2007b). Meanwhile, with the increase of surfactant loading, two mass losses occurred at 320–440 and 440–540 °C, respectively. These two mass losses are attributed to the further decomposition of the residual organic carbonaceous residue, which was formed in the first stage at ~266 °C (Vaia et al., 1994; Xie et al., 2001).

4. Conclusions

In this study, HEVrm were synthesized using EVrm at different HDTMAB concentrations. The intercalation of HDTMAB into EVrm interlayer space is very different from the case into Mt. That is, a one-stepped increase of the basal spacing of HEVrm was observed in this study, instead of a gradual stepwise increase of the basal spacing as reported for OMt in literature. The present study demonstrates that the intercalation of Vrm interlayers is not homogeneous, i.e., only part of the interlayer spaces were intercalated by HDTMAB at low surfactant concentration. With the increase of surfactant concentration in the preparation solution, more and more interlayer spaces were occupied and reached a complete modification state at last. The one-stepped increase probably should be attributed to the heterogeneous charge density layer by layer as well as the high layer charge density in Vrm. The interlayer height of the resulting HEVrm suggests that a paraffin-monolayer arrangement model was adopted by the intercalated surfactant within the Vrm interlayer space.

With an increase of surfactant loading, both the desorption temperature of the surface adsorbed water and the mass loss of the interlayer water associated with the interlayer cations dramatically decrease, indicating the replacement of the original interlayer cations by cationic surfactant and an increase of surface hydrophobicity of HEVrm, in comparison with the original EVrm. Different from the case of OMt, the decomposition temperature of the intercalated surfactant in the obtained HEVrm is very similar to that of neat surfactant. This suggests that the protection of the clay mineral layers for the thermal stability of the intercalated surfactant only occurs in OC with relatively small interlayer height. These findings are significantly important for the preparation and application of HEVrm, which have larger basal spacing at relatively low surfactant loading in comparison with OMt.

Table 3
Mass losses of EVrm, HDTMAB, and HEVrm at different stages deduced from TG curves.

	Mass loss (%)		
	Desorption (adsorbed water)	Desorption (interlayer water)	Decomposition (surfactant)
Samples	30–150 °C	150–210 °C	210–500 °C
EVrm	6.9	–	–
HDTMAB	–	–	99.9
$HEVrm_{0.2}$	7.0	3.0	6.1
$HEVrm_{0.4}$	8.1	3.0	10.4
$HEVrm_{0.6}$	6.1	3.5	14.5
$HEVrm_{0.8}$	6.5	3.8	18.1
$HEVrm_{1.0}$	6.3	–	22.4
$HEVrm_{1.5}$	5.8	–	24.6
$HEVrm_{2.0}$	5.1	–	26.1
$HEVrm_{3.0}$	5.4	–	26.2

Acknowledgements

This work was financially supported by the National Natural Science Foundation of China (grant nos. 41402038; 41322014), Team Project of Natural Science Foundation of Guangdong Province, China (grant no. S2013030014241), Cooperative Research Foundation of Guangdong Provincial Key Laboratory of Mineral Physics and Materials (GLMPM-008), and National Youth Top-notch Talent Support Program. This is contribution No.IS-2258 from GIGCAS.

References

Bergaya, F., Lagaly, G., 2011. Intercalation processes of layered minerals. In: Brigatti, M.F., Mottana, A. (Eds.), Layered Mineral Structure and Their Application in Advanced Technology, EMU, Notes in Mineralogy vol. 11. European Mineralogical Union and the Mineralogical Society of Great Britain, London, pp. 259–284.

Bergaya, F., Lagaly, G., 2013. General introduction: clays, clay minerals, and clay science. In: Bergaya, F., Lagaly, G. (Eds.), Handbook of Clay Science, Developments of Clay Science vol. 5A. Elsevier, Amsterdam, pp. 1–19.

Brigatti, M.F., Theng, B.K.G., 2013. Structure and mineralogy of clay minerals. In: Bergaya, F., Lagaly, G. (Eds.), Handbook of Clay Science, Developments in Clay Science vol. 5A. Elsevier, Amsterdam, pp. 20–81.

Cai, Y.H., 2012. Preparation of organo-vermiculite by modification with hexadecyltrimethylammonium bromide under microwave irradiation. Asian J. Chem. 24, 252–254.
Dultz, S., An, J.H., Riebe, B., 2012. Organic cation exchanged montmorillonite and vermiculite as adsorbents for Cr(VI): effect of layer charge on adsorption properties. Appl. Clay Sci. 67–68, 125–133.
He, H.P., Guo, J.G., Zhu, J.X., Hu, C., 2003. ^{29}Si and ^{27}Al MAS NMR study of the thermal transformations of kaolinite from North China. Clay Clay Miner. 38, 551–559.
He, H.P., Frost, R.L., Deng, F., Zhu, J.X., Wen, X., Yuan, P., 2004a. Conformation of surfactant molecules in the interlayer of montmorillonite studied by ^{13}C MAS NMR. Clay Clay Miner. 52, 350–356.
He, H.P., Ray, F.L., Zhu, J.X., 2004b. Infrared study of HDTMA$^+$ intercalated montmorillonite. Spectrochim. Acta A 60, 2853–2859.
He, H.P., Ding, Z., Zhu, J.X., Yuan, P., Xi, Y.F., Yang, D., Frost, R.L., 2005a. Thermal characterization of surfactant-modified montmorillonites. Clay Clay Miner. 53, 287–293.
He, H.P., Galy, J., Gerard, J.F., 2005b. Molecular simulation of the interlayer structure and the mobility of alkyl chains in HDTMA$^+$/montmorillonite hybrids. J. Phys. Chem. B 109, 13301–13306.
He, H.P., Yuan, P., Guo, J.G., Zhu, J.X., Hu, C., 2005c. The influence of random defect density on the thermal stability of kaolinites. J. Am. Ceram. Soc. 88, 1017–1019.
He, H.P., Zhou, Q., Martens, W.N., Kloprogge, T.J., Yuan, P., Xi, Y.F., Zhu, J.X., Frost, R.L., 2006. Microstructure of HDTMA$^+$-modified montmorillonite and its influence on sorption characteristics. Clay Clay Miner. 54, 689–696.
He, H.P., Ma, Y.H., Zhu, J.X., Yuan, P., Qing, Y.H., 2010. Organoclays prepared from montmorillonites with different cation exchange capacity and surfactant configuration. Appl. Clay Sci. 48, 67–72.
He, H.P., Ma, L.Y., Zhu, J.X., Frost, R.L., Theng, B.K.G., Bergaya, F., 2014. Synthesis of organoclays: a critical review and some unresolved issues. Appl. Clay Sci. 100, 22–28.
Hedley, C.B., Yuan, G.H., Theng, B.K.G., 2007. Thermal analysis of montmorillonites modified with quaternary phosphonium and ammonium surfactants. Appl. Clay Sci. 35, 180–188.
Holesova, S., Stembirek, J., Bartosova, L., Prazanova, G., Valaskova, M., Samlikova, M., Pazdziora, E., 2014. Antibacterial efficiency of vermiculite/chlorhexidine nanocomposites and results of the in vivo test of harmlessness of vermiculite. Mater. Sci. Eng. C 42, 466–473.
Huo, X.X., Wu, L.M., Liao, L.B., Xia, Z.G., Wang, L.J., 2012. The effect of interlayer cations on the expansion of vermiculite. Powder Technol. 224, 241–246.
Liu, B., Wang, X.Y., Yang, B., Sun, R.C., 2011. Rapid modification of montmorillonite with novel cationic Gemini surfactants and its adsorption for methyl orange. Mater. Chem. Phys. 130, 1220–1226.
Ma, L.Y., Zhu, J.X., He, H.P., Tao, Q., Zhu, R.L., Shen, W., Theng, B.K.G., 2014. Al_{13}-pillared montmorillonite modified by cationic and zwitterionic surfactants: a comparative study. Appl. Clay Sci. 101, 327–334.
Ma, L.Y., Zhu, J.X., He, H.P., Xi, Y.F., Zhu, R.L., Tao, Q., Liu, D., 2015. Thermal analysis evidence for the location of zwitterionic surfactant on clay minerals. Appl. Clay Sci. 112, 62–67.
Mittal, V., 2012a. Modification of montmorillonites with thermally stable phosphonium cations and comparison with alkylammonium montmorillonites. Appl. Clay Sci. 56, 103–109.
Mittal, V., 2012b. Surface modification of layered silicates. II. Factors affecting thermal stability. Philos. Mag. 92, 4518–4535.
Park, Y., Ayoko, G.A., Kristof, J., Horvath, E., Frost, R.L., 2012. A thermoanalytical assessment of an organoclay. J. Therm. Anal. Calorim. 107, 1137–1142.
Perez-Maqueda, L.A., Balek, V., Poyato, J., Perez-Rodriquez, J.L., Subrt, J., Bountsewa, I.M., Beckman, I.N., Malek, Z., 2003. Study of natural and ion exchanged vermiculite by emanation thermal analysis, TG, DTA and XRD. J. Therm. Anal. Calorim. 71, 715–726.
Placha, D., Rosenbergova, K., Slabotinsky, J., Mamulova Kutlakova, K., Studentova, S., Simha Martynkova, G., 2014. Modified clay minerals efficiency against chemical and biological warfare agents for civil human protection. J. Hazard. Mater. 271, 65–72.
Tjong, S.C., Meng, Y.Z., 2003. Impact-modified polypropylene/vermiculite nanocomposites. J. Polym. Sci. B Polym. Phys. 41, 2332–2341.
Vaia, R.A., Teukolsky, R.K., Giannelis, E.P., 1994. Interlayer structure and molecular environment of alkylammonium layered silicates. Chem. Mater. 6, 1017–1022.
Valaskova, M., Martynkova, G.S., Matejka, V., Barabaszova, K., Plevova, E., Merinska, D., 2009. Organovermiculite nanofillers in polypropylene. Appl. Clay Sci. 43, 108–112.
Walker, G., 1949. Water layers in vermiculite. Nature 163, 726.
Wang, L., Wang, X., Chen, Z.Y., Ma, P.C., 2013. Effect of doubly organo-modified vermiculite on the properties of vermiculite/polystyrene nanocomposites. Appl. Clay Sci. 75–76, 74–81.
Wang, Y.B., Su, X.L., Lin, X.Q., Zhang, P., Wen, K., Zhu, J.X., He, H.P., 2015. The non-micellar template model for porous clay heterostructures: a perspective from the layer charge of base clay. Appl. Clay Sci. 116, 102–110.
Xi, Y.F., Zhou, Q., Frost, R.L., He, H.P., 2007a. Thermal stability of octadecyltrimethylammonium bromide modified montmorillonite organoclay. J. Colloid Interface Sci. 311, 347–353.
Xi, Y.F., Frost, R.L., He, H.P., 2007b. Modification of the surfaces of Wyoming montmorillonite by the cationic surfactants alkyl trimethyl, dialkyl dimethyl, and trialkyl methyl ammonium bromides. J. Colloid Interface Sci. 305, 150–158.
Xie, W., Gao, Z.M., Pan, W.P., Hunter, D., Singh, A., Vaia, R., 2001. Thermal degradation chemistry of alkyl quaternary ammonium montmorillonite. Chem. Mater. 13, 2979–2990.
Xie, W., Xie, R.C., Pan, W.P., Hunter, D., Koene, B., Tan, L.S., Vaia, R., 2002. Thermal stability of quaternary phosphonium modified montmorillonites. Chem. Mater. 14, 4837–4845.
Zhu, J.X., He, H.P., Guo, J.G., Yang, D., Xie, X.D., 2003. Arrangement models of alkylammonium cations in the interlayer of HDTMA$^+$ pillared montmorillonites. Chin. Sci. Bull. 48, 368–372.
Zhu, J.X., He, H.P., Zhu, L.Z., Wen, X.Y., Deng, F., 2005. Characterization of organic phases in the interlayer of montmorillonite using FTIR and ^{13}C NMR. J. Colloid Interface Sci. 286, 239–244.
Zhu, R.L., Zhu, L.Z., Zhu, J.X., Xu, L.H., 2008. Structure of cetyltrimethylammonium intercalated hydrobiotite. Appl. Clay Sci. 42, 224–231.
Zhu, J.X., Wang, T., Zhu, R.L., Ge, F., Wei, J.M., Yuan, P., He, H.P., 2011. Novel polymer/surfactant modified montmorillonite hybrids and the implications for the treatment of hydrophobic organic compounds in wastewaters. Appl. Clay Sci. 51, 317–322.
Zhu, J.X., Shen, W., Ma, Y.H., Ma, L.Y., Zhou, Q., Yuan, P., Liu, D., He, H.P., 2012a. The influence of alkyl chain length on surfactant distribution within organo-montmorillonites and their thermal stability. J. Therm. Anal. Calorim. 109, 301–309.
Zhu, R.L., Chen, W.X., Liu, Y., Zhu, J.X., Ge, F., He, H.P., 2012b. Application of linear free energy relationships to characterizing the sorptive characteristics of organic contaminants on organoclays from water. J. Hazard. Mater. 233-234, 228–234.